Egyptian Journal of Radiology and Nuclear Medicine

RESEARCH

Open Access

Role of intravoxel incoherent motion diffusion-weighted MRI in differentiation of renal cell carcinoma subtypes

Amira R. Mahmoud[1*], Nehad Fouda[2], Eman Mohamed Helmy[2] and Ali Elsorougy[1]

Abstract

Background Renal cell carcinoma is the most fatal form of renal tumors, representing about ninety percent of all renal cancers. There are different variations in prognosis among various histological types of RCC. In recent years, there has been a greater emphasis on differentiating between RCC subtypes. Evaluation of different subtypes of renal cell carcinoma using intravoxel incoherent motion (IVIM) diffusion-weighted MRI is the aim of this study.

Results Clear cell renal cell carcinoma (CCRCCs) showed highest f and D values, followed by chromophobe renal cell carcinoma (ChRCCs), while papillary renal cell carcinoma (PRCCs) had the lowest values. CCRCCs had significantly different D and f values compared to non-clear types (PRCC and ChRCC) ($P < 0.05$). The D* values of CCRCC were the highest, PCRCC had intermediate values, while ChRCCs had the lowest values ($P < 0.05$). The D* values of ChRCCs demonstrated significant difference when compared to both CCRCCs and PRCCs ($P < 0.05$). The cutoff points of D, D^* and f parameters for distinguishing CCRCCs from non-clear cell types (ChRCCs and PRCC) were 0.835, 0.0355 and 0.335, respectively, yielding specificities of 97.2%, 83.3% and 76.5% and sensitivities of 100%, 57.5% and 72.7%, respectively.

Conclusion Intravoxel incoherent motion (IVIM) can be utilized to distinguish renal cell carcinoma subtypes.

Keywords Kidney, Renal cell carcinoma, IVIM MRI

Background

Renal cell carcinoma (RCC) is a multiple variety of tumors that originates from the epithelium of the renal tubules. It is considered as a group of illness with discrete histological types, molecular and genetic variations with distinct clinical prognosis [1].

Clear cell, papillary and chromophobe RCCs are the most predominant subtypes of RCC, constituting approximately 75%, 15% and 5% of RCCs cases, respectively. According to the 2004 WHO classification system [2], clear cell carcinomas type typically exhibits a less favorable prognosis with a five-year survival rate ranging from 44 to 69% [3].

Differentiation of renal masses is useful in distinguishing those that require active surveillance or ablation from those requiring surgery without the need for biopsy [4]. Histological classification of RCC is performed preoperative by invasive methods through percutaneous biopsy. Recently, a large number of studies have documented the value of imaging in the non-invasive evaluation of different RCC subtypes [5].

Non-invasive techniques, such as MRI, have been thoroughly detailed in the assessment of common frequent subtypes of RCC [6]. Both diffusion-weighted imaging (DWI) and apparent diffusion coefficient (ADC) measurements were extensively utilized in the characterization

*Correspondence:
Amira R. Mahmoud
dramira5122018@gmail.com
[1] Radiology and Medical Imaging, Urology and Nephrology Center, Mansoura University, Mansoura, Egypt
[2] Diagnostic Radiology and Medical Imaging, Faculty of Medicine, Mansoura University, Mansoura, Egypt

as well as identification of renal masses [7, 8]. However, the ADC is determined with a monoexponential model and does not adequately reflect the diffusion factor of tissues as it involves the impacts of perfusion (the capillaries microcirculation of blood) and diffusion (water molecules movement inside tissue) [9].

Intravoxel incoherent motion (IVIM) DWI, initially documented by Le Bihan et al., uses the biexponential model with several b values to calculate both tissues diffusion and perfusion, independently [9]. Main IVIM parameters include true diffusion coefficient (D), pseudo-diffusion (D*) and perfusion fraction (f) that represent the tissue true molecular diffusion, perfusion of blood capillary microcirculation and the microcapillary perfusion fraction, respectively [9, 10].

IVIM MRI is sensitive to both molecular diffusion in tissues and to microcirculation (perfusion) based on the assumption that the flow of blood through capillaries mimics a diffusion process, due to the pseudo-random organization of capillaries in tissue [11]. Microcirculation contributes greatly to the diffusion-weighted MRI signal together with genuine water molecule diffusion in tissues [12, 13].

A key advantage of IVIM MRI is ability to give quantitative data about microcirculation without using contrast agents, a significant benefit in terms of price, acquisition times and suitability for patients who are contraindicated to receive gadolinium-based contrast agents [14, 15].

Methods

- This prospective study was done from May 2023 to December 2023. All cases were referred to our radiology department at urology and nephrology center from the clinic within the same center. Our study received permission by the institutional board of ethics, and each patient gave his informed consent after being fully informed about the benefits and hazards of the procedure. There were no other obvious hazards to the patients in this study.
- *Inclusion criteria* Patients over the age of eighteen years who had solid renal mass parenchymal in origin that have been identified by CT or US.
- *Exclusion criteria* Patients who are contraindicated for MRI study (like patient with metallic prostheses or pacemakers), cases who refused consent and cases with no histology results

MRI technique

MRI examination was performed for each patient using a 3 Tesla MRI scanner (Phillips, Ingenia 3 T, Best, The Netherlands). Phased-array body coil using M-Dixon program was utilized in our procedure, and imaging was done in the supine position including these sequences: (T2WI, fat-suppressed T1W sequences, DWI, IVIM). As regards the IVIM, in the axial or coronal planes, we applied single-shot echo-planar imaging sequence using a respiratory belt with eight b values (0, 200, 400, 600, 800, 1000, 1200 and 1400 s/mm^2). Other parameters were: 24 slices covering both kidneys, (TE) = 33.2 × 86.6 ms, (TR) = 1000 ms, matrix = 96 × 128, FOV = 36 × 36 cm. The mean acquisition time of IVIM sequence was 16.6 + 3.2 min.

Image analysis

The DICOM pictures were sent to the vendor-supplied workstation (Intellispace portal Workspace 6.0.1 Philips Medical Systems Netherlands B.V). The procedure was done without knowledge of the pathology results. Using IVIM protocol, we got measurements for D, D* and f. ROIs of the lesion (100–225 mm^2) were manually drawn trying to avoid aliasing artifacts appeared in an image, calcification inside the mass and cystic degeneration. We obtained three measurements for each parameter, and the average measurement was taken.

Statistical analysis and data interpretation

Version 25 of the SPSS program (SPSS Inc., PASW statistics for windows version 25. Chicago: SPSS Inc.) was used to analyze the data. Numbers and percentages were used to describe the qualitative data. After determining the normalcy of the quantitative data using the Kolmogrov–Smirnov or Shapiro–Wilk tests, the data were presented using the mean ± standard deviation for normally distributed data. The results were evaluated for significance at the (≤ 0.05) level.

When comparing more than two independent groups, the one-way ANOVA test was utilized and the post hoc Tukey test was applied to identify pair-wise comparisons. The best cutoff point was determined by calculating the validity (sensitivity & specificity) of continuous variables using the receiver operating characteristics curve (ROC curve). Using cross-tabulation, predictive values and accuracy are evaluated.

Pathological analysis

Final diagnosis by histopathology was obtained after excision of renal masses surgically by either partial or radical nephrectomy.

Results

Seventy-six patients with renal cell carcinomas confirmed by histology were included in our prospective study (35 females and 41 males). Their age range was (29–77) years with average age that was 53.13 years. We observed no

significant differences for either age ($p=0.81$) or sex ($p=0.34$). The distribution of their pathology was 40 clear cell RCCs (52.6%), 22 papillary RCCs (28.9%) and 14 chromophobe RCCs (18.5%) (Fig. 1).

D values were highest for CCRCCs ($1.44\pm0.19\times10^{-3}mm^2/s$) followed by ChRCC ($0.751\pm0.054\times10^{-3}mm^2/s$) and lowest for PRCCs ($0.575\pm0.043\times10^{-3}mm^2/s$) (Figs. 2, 3). The D parameter showed also high statistically significant difference in differentiating clear cell type from non-clear cell types including both chromophobe & papillary types, $p<0.001$ for both (Table 1). The area under curve for Diffusion coefficient (D) was excellent (AUC = 1.0), and the cutoff point of D value was ≥ 0.835 for distinguishing CCRCCs from non-clear cell types (ChRCCs and PRCCs) with sensitivity of 100% and specificity of 97.2% (Table 2), (Figs. 6, 7, 8).

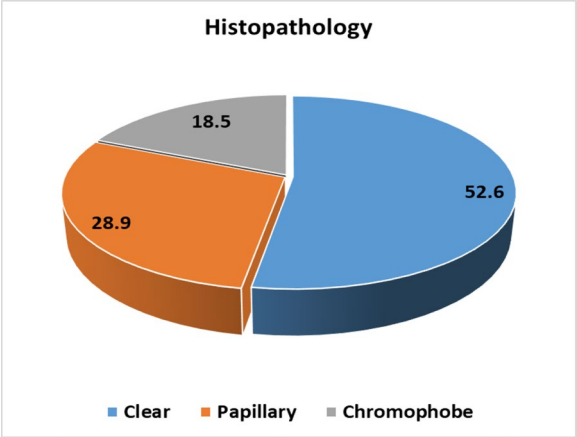

Fig. 1 Histopathology of the studied cases

Regarding the D* parameter, CCRCCs also had the highest D* values (0.035 ± 0.006 mm^2/s) followed by PRCCs (0.033 ± 0.002 mm^2/s) and lowest for ChRCCs (0.022 ± 0.004 mm^2/s) (Figs. 2, 4). Statistically significant difference was detected among CCRCCs & ChRCCs types and between PRCCs & ChRCCs ($P<0.001$ for both), but no statistically significant difference was detected between CCRCCs & PRCCs ($p=0.084$) (Table 1). AUC for pseudo-diffusion (D*) is good (AUC = 0.745), with the best detected cutoff point for differentiating CCRCCs from non-clear cell types (ChRCCs and PRCCs) that is ≤ 0.0355 yielding sensitivity of 57.5% and specificity 83.3% (Table 2), (Figs. 6, 7, 8).

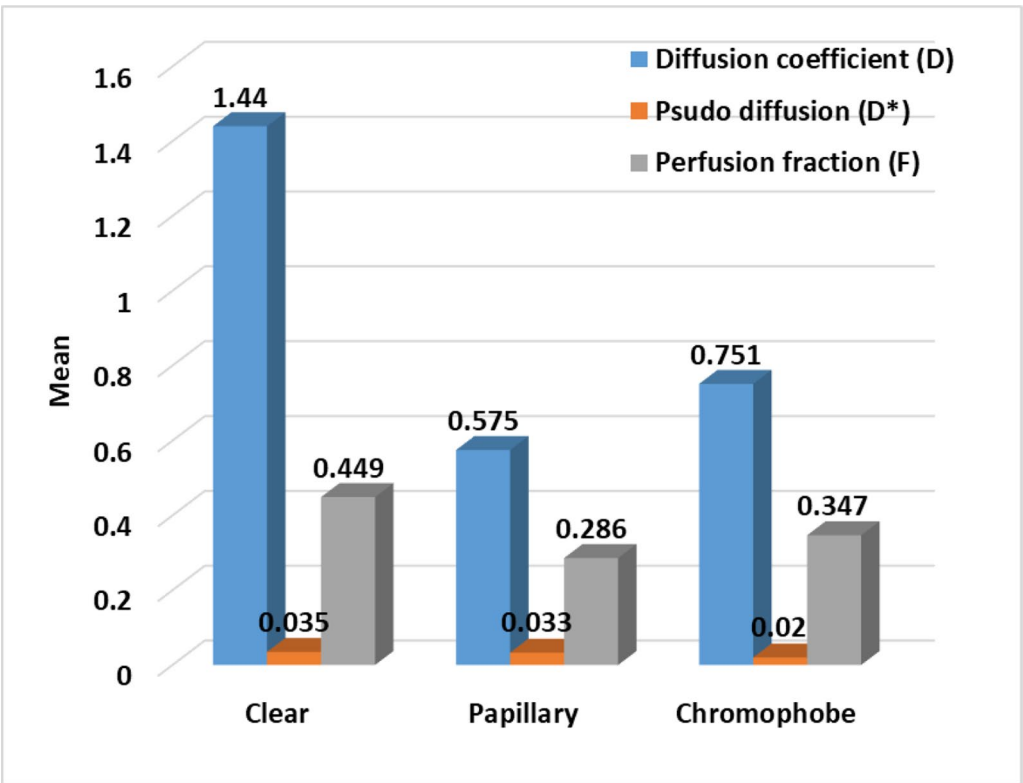

Fig. 2 The mean values for D, D* and f among the three subtypes, CCRCC, PRCC and ChRCCs. D diffusion coefficient, D*pseudo-diffusion, f perfusion fraction, CCRCC clear cell renal cell carcinoma, PRCC papillary renal cell carcinoma, ChRCCs chromophobe renal cell carcinoma

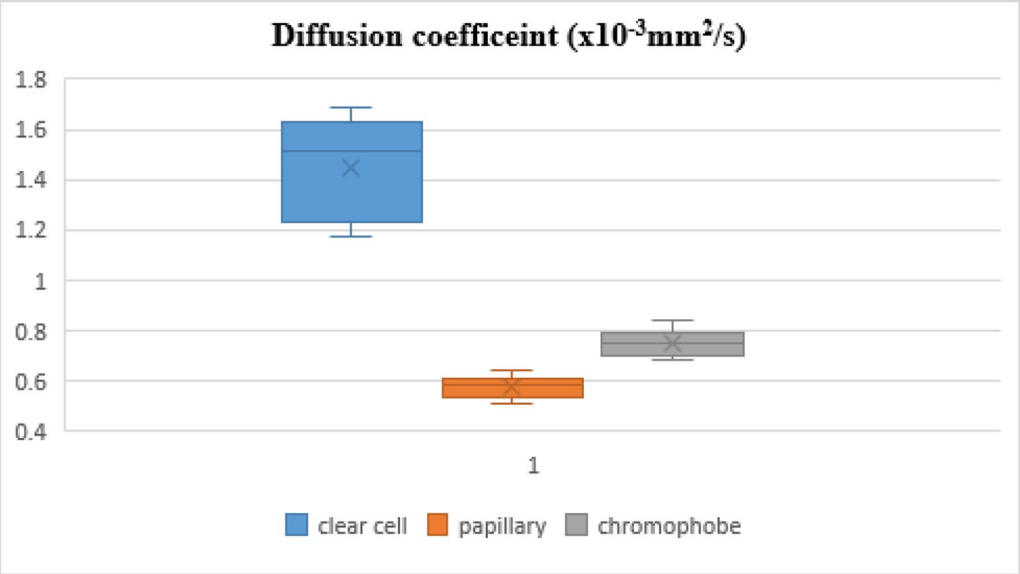

Fig. 3 Boxplot shows the difference between clear cell, papillary and chromophobe RCCs measurements according to the D parameter within the studied groups. The D values were highest for CCRCC ($1.44 \pm 0.19 \times 10^{-3}$mm^2/s) followed by ChRCCs ($0.751 + 0.054 \times 10^{-3}$mm^2/s) and lowest for PRCC ($0.575 + 0.043 \times 10^{-3}$mm^2/s). D diffusion coefficient, CCRCC clear cell renal cell carcinoma, ChRCCs chromophobe renal cell carcinoma, PRCC papillary renal cell carcinoma

Table 1 Relation between radiological findings as regard D, D* and f and histopathology among studied cases

	Histopathology			Within-group significance
	Clear N = 40	Papillary N = 22	Chromophobe N = 14	
D ($\times 10^{-3}$mm^2/s)	1.44 ± 0.19	0.575 ± 0.043	0.751 ± 0.054	P1 < 0.001* P2 < 0.001* P3 < 0.001*
D*(mm^2/s)	0.035 ± 0.006	0.033 ± 0.002	0.022 ± 0.004	P1 = 0.084 P2 < 0.001* P3 < 0.001*
f (%)	0.449 ± 0.16	0.286 ± 0.045	0.347 ± 0.07	P1 < 0.001* P2 = 0.008* P3 = 0.139

Parameters described as mean ± SD.*statistically significant, P1: difference between clear & papillary carcinoma group, P2: difference between clear and chromophobe, P3: difference between papillary & chromophobe

Table 2 Validity of D, D* and f in differentiating clear cell type (CCRCC) from non-clear cell types (ChRCCs & PRCC)

	AUC (95%CI)	P value	Cutoff point	Sensitivity %	Specificity %
D	1.0 (1.0–1.0)	< 0.001*	≥ 0.835	100.0	97.2
D*	0.745 (0.635–0.856)	< 0.001*	≥ 0.0355	57.5	83.3
f	0.823 (0.728–0.917)	< 0.001*	≥ 0.335	72.7	76.5

The f values were highest for CCRCCs (0.449 ± 0.16%) followed by ChRCCs (0.347 ± 0.07%) and lowest for PRCCs (0.286 ± 0.045%) (Figs. 2, 5). Statistically significant difference was detected between CCRCCs & PRCCs (P1 < 0.001) and between CCRCCs & ChRCCs (P2 < 0.008), but no statistically significant difference was detected between ChRCCs & PRCCs (P3 = 0.139) (Table 1). Area under curve for perfusion fraction (f)

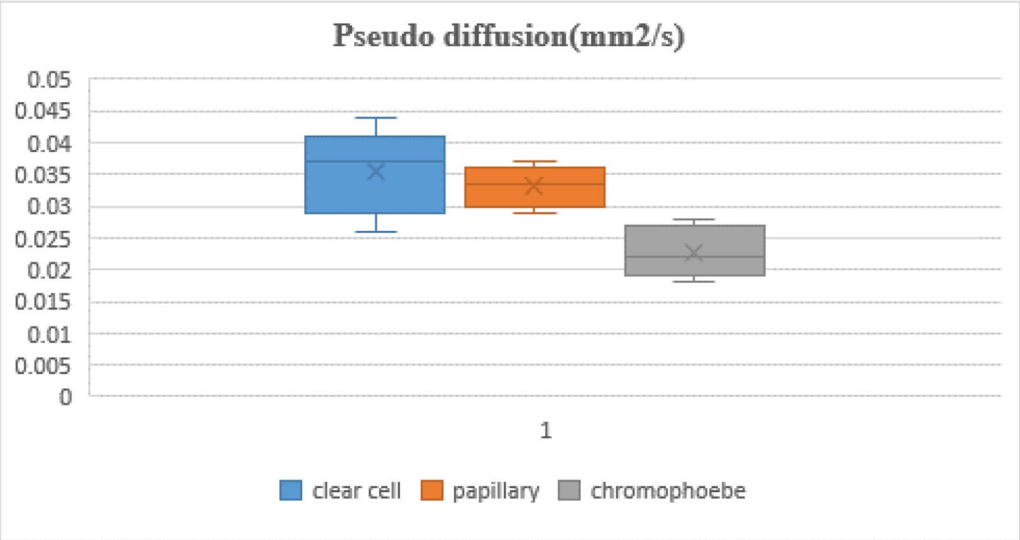

Fig. 4 Boxplot shows the difference between clear cell, papillary and chromophobe RCCs measurements according to the D* parameter within the studied groups. The D* values were highest for CCRCCs (0.035 ± 0.006 mm^2/s) followed by PRCCs (0.033 ± 0.002 mm^2/s) and lowest for ChRCCs (0.022 ± 0.004 mm^2/s). D* diffusion coefficient, CCRCC clear cell renal cell carcinoma, ChRCC chromophobe renal cell carcinoma, PRCC papillary renal cell carcinoma

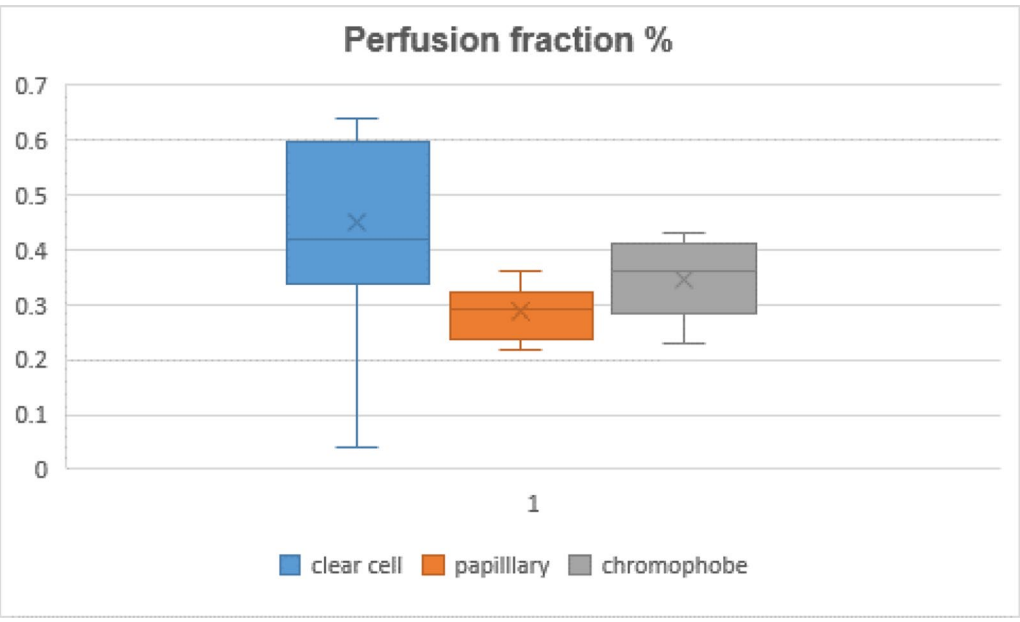

Fig. 5 Boxplot shows the difference between clear cell, papillary and chromophobe RCCs measurements according to the f parameter within the studied groups. The f values were highest for CCRCCs (0.449 ± 0.16%) followed by ChRCCs (0.347 ± 0.07%) and lowest for PRCCs (0.286 ± 0.045%). f perfusion fraction, CCRCC clear cell renal cell carcinoma, ChRCC chromophobe renal cell carcinoma, PRCC papillary renal cell carcinoma

was excellent (AUC = 0.823), with the best detected cut-off point for differentiating CCRCCs from non-clear cell types (ChRCCs and PRCCs) that is ≤ 0.355 yielding sensitivity of 72.7%, specificity 76.5% (Table 2), (Figs. 6, 7, 8).

Discussion

Renal cell carcinoma is the most fatal form of renal tumors, representing about ninety percent of all renal cancers, and its incidence increases annually by about

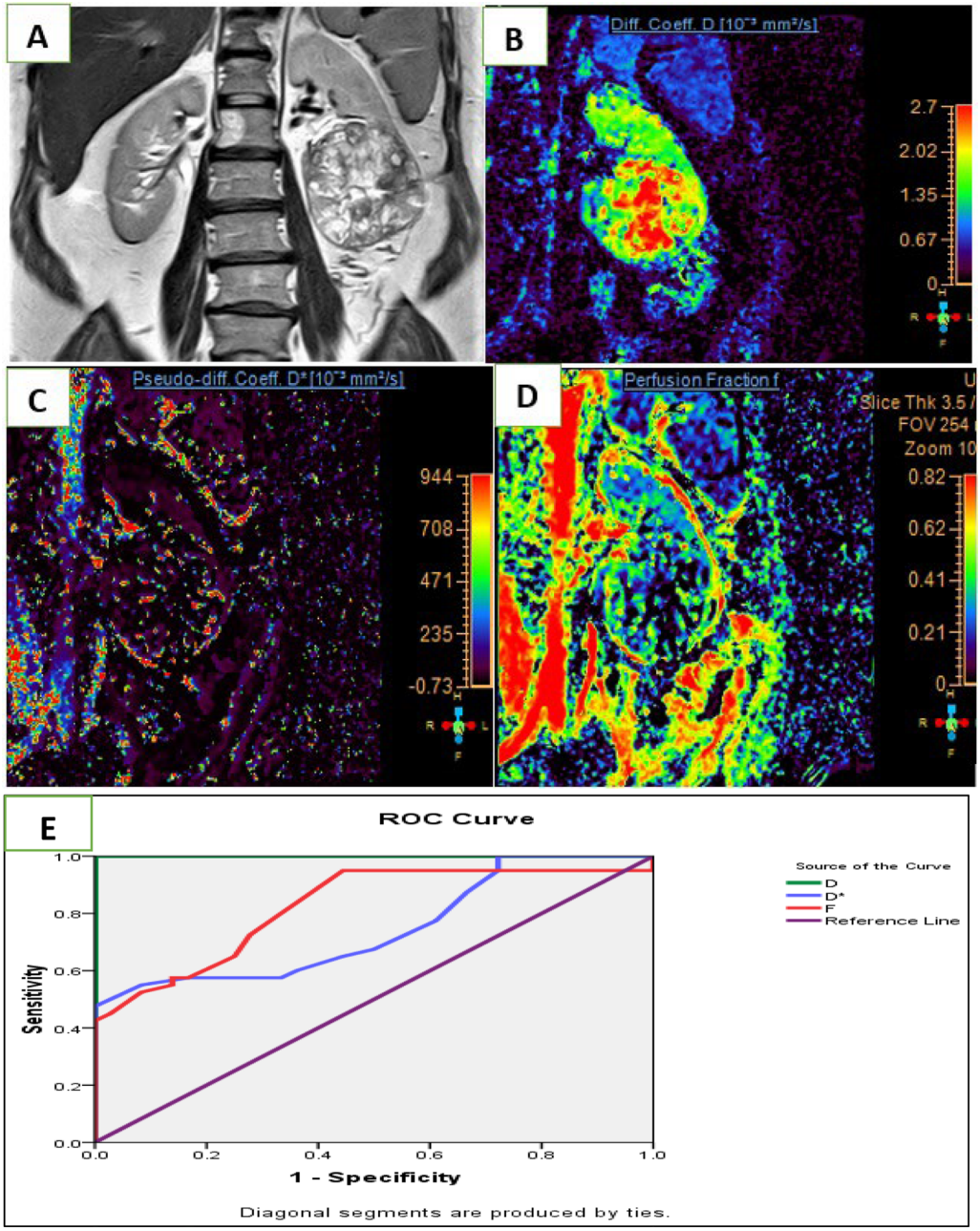

Fig. 6 A 63-year-old male patient presented with left lower polar soft tissue mass confirmed as clear cell RCC by histopathology. **A** Coronal T2WI showing heterogenous SI of the renal mass. **B**–**D** Showing D, D* and f maps with measured values as 1.23 × 10–3 mm^2/s, 0.028 mm^2/s and 0.43%, respectively. **E** ROC curve of D, D* & F in differentiating clear cell RCC from non-clear cell types (ChRCC & PRCC)

2–3% [16]. The most predominant subtype of RCC is clear cell type, representing about 75%. It is also the worst form of RCCs regarding its prognosis with five-year survival rate ranging from 44 to 69% [3, 17].

Multiparametric MRI has recently become the most reliable method for differentiation of renal tumors, yet other advanced MRI techniques are still required to evaluate renal tumor subtypes. ADC is a quantitative method determined from MR-DWI images that is affected by numerous physiological and pathological states of the renal system [18].

IVIM can be done without the need of contrast agents' injection to offer a distinctive image of the tissue perfusion. The proportion of tumor tissue cellularity and

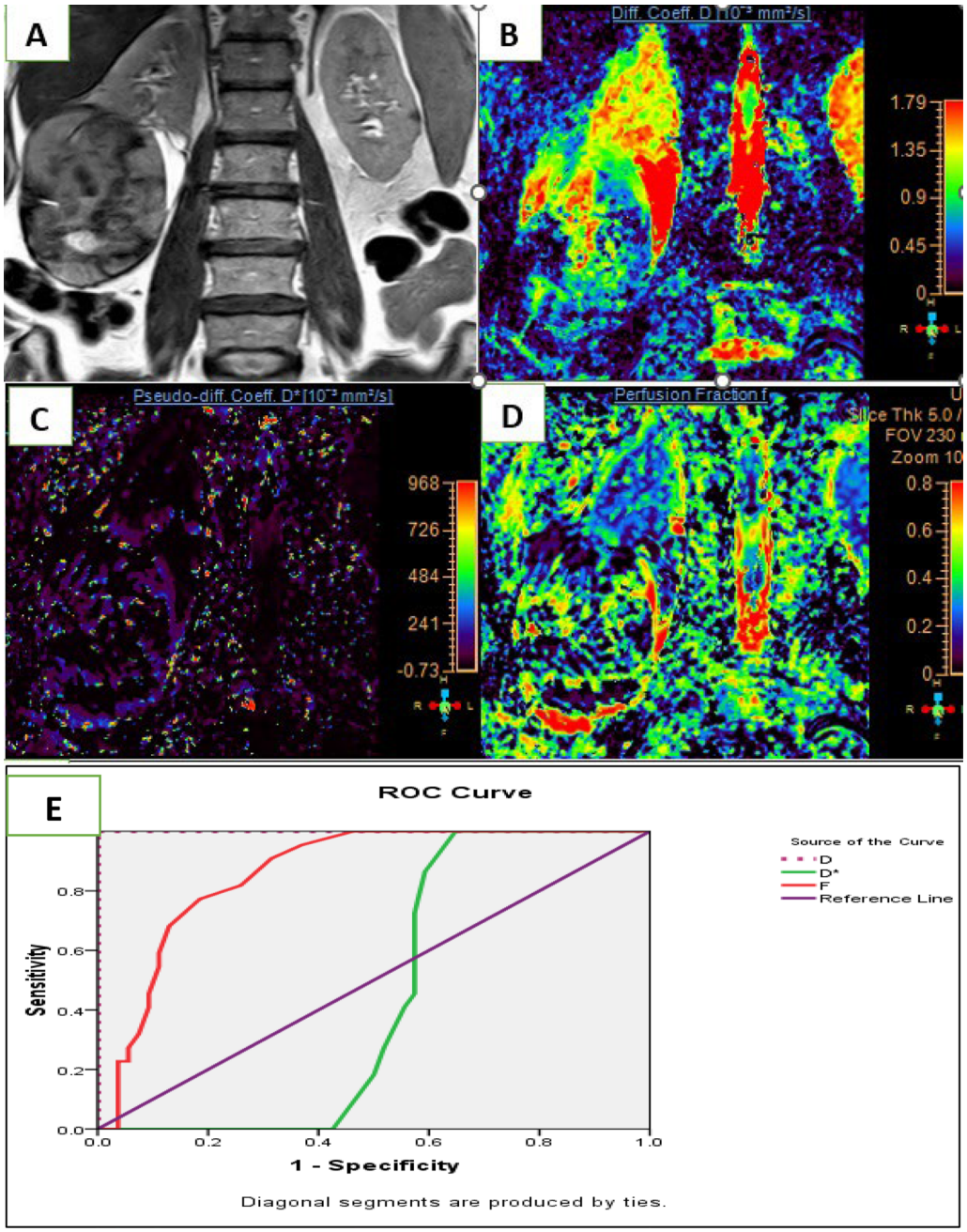

Fig. 7 A 52-year-old male patient presented with right lower polar soft tissue mass confirmed as papillary RCC by histopathology. **A** Coronal T2WI showing heterogenous SI of the renal mass. **B**–**D** Showing D, D* and f maps with measured values as 0.53 × 10–3 mm^2/s, 0.031 mm^2/s and 0.22%, respectively. **E** ROC curve of D, D* & f in differentiating papillary RCC from other types (CCRCC & ChRCC)

vascularity varies between renal tumor types; therefore, the IVIM parameters including D, D* and f can represent different issues that operate within ADC and can offer accurate and sensitive assessment of renal masses [13].

The random microscopic movement of water molecules in extra- or intracellular spaces as well as in the blood microcirculation that arises in each voxel on MR images is reflected by IVIM [9]. IVIM theory suggested that a number of tissue characteristics, such as the existence of restricting barriers inside the tissue, the fluid consistency in which the spinning molecules are spreading, the speed and fractional volume of perfusing spins all have an impact on perfusion and diffusion [11].

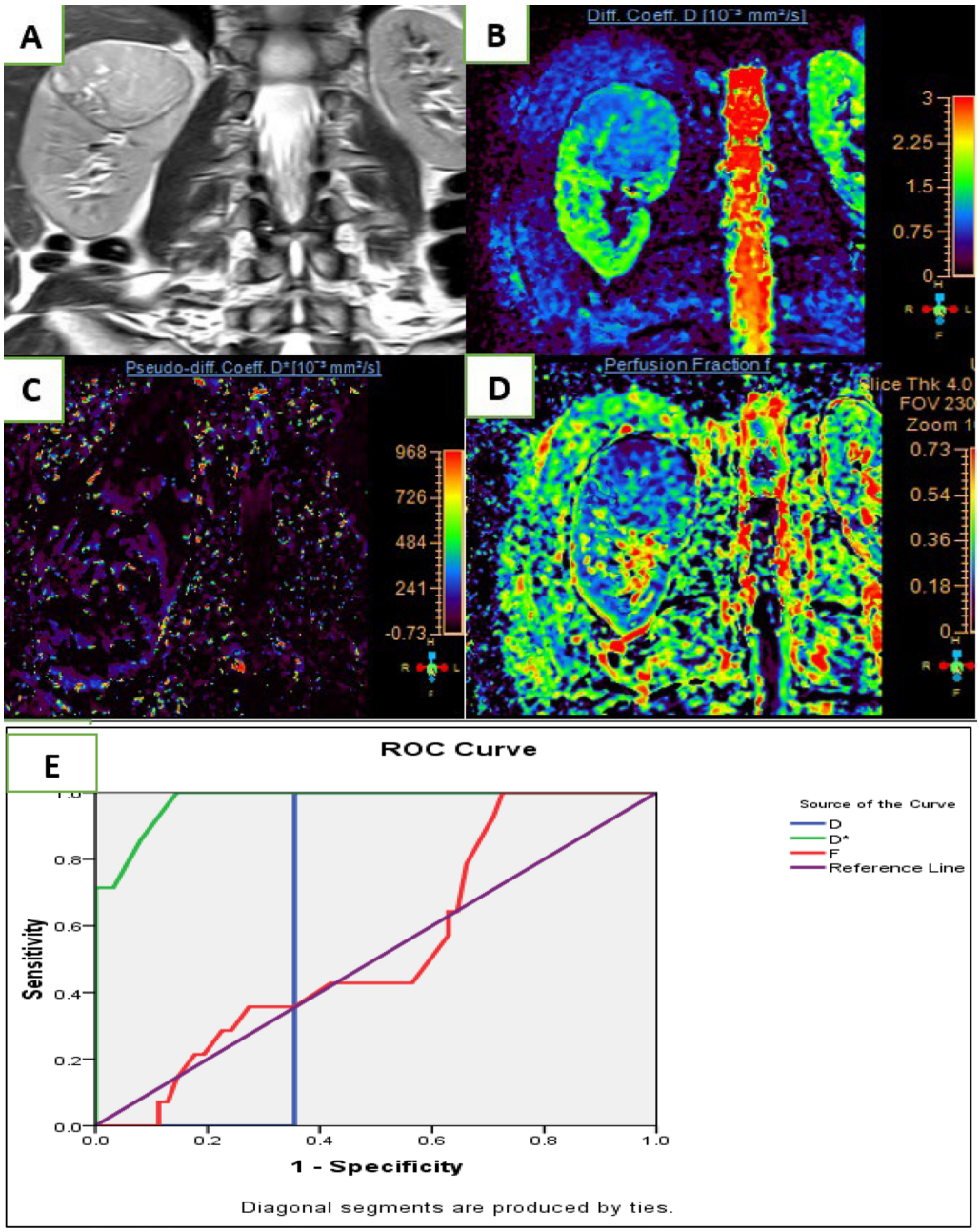

Fig. 8 A 48-year-old male patient presented with right upper polar soft tissue mass confirmed as chromophobe RCC by histopathology. **A** Coronal T2WI showing intermediate SI of the renal mass. **B**–**D** Showing D, D* and f maps with measured values as 0.73 × 10–3 mm^2/s, 0.023 mm^2/s and 0.29%, respectively. **E** ROC curve of D, D* & f in differentiating chromophobe cell RCC from other types (CCRCC & PRCC)

Assessment of renal tumors is beneficial in determining masses that require surgical excision with no further assessment by biopsy from masses that need active surveillance or ablation [19]. Therefore, we conducted this prospective study, with the primary aim that is to assess role of IVIM in renal cell carcinomas characterization and differentiation in correlation with histopathology subtypes.

In our study, CCRCCs showed the highest D values followed by ChRCCs and lowest for PRCCs. The D parameter showed also high significant statistical difference between clear cell type and both chromophobe &

papillary types, $P<0.001$ for both with the best detected cutoff value for discrimination of clear cell types versus non-clear cell types is ≥ 0.835 with (AUC = 1.0) yielding sensitivity of 100.0% and specificity 97.2%. Tissue cellularity and perfusion have an impact on the D values. It was reported that lower D values have been correlated to greater cellularity in several studies [20]. Also, the lower D values could be caused by the viscosity of the tumor or mechanical restriction of water diffusion by barriers such cell membranes. The cells of clear cell RCC are rich in phospholipids, cholesterol and neutral lipids. Moreover, tumor cells of CCRCCs are separated by interstitial spaces and have hemorrhagic and cystic areas, which allowed water to spread freely [21].

As regard the f parameter, it nearly showed the same results as the D parameter, its values were high within CCRCCs, moderate within ChRCCs and low within PRCC, but we found significant statistical difference among CCRCCs & PRCCs ($P<0.001$), as well as CCRCCs & ChRCCs ($P<0.008$). But significant statistical difference noticed among PRCCs & ChRCCs ($P=0.139$) with best detected cutoff value for discrimination of clear cell types versus non-clear cell types that is ≤ 0.355 (AUC = 0.823), resulting in sensitivity about 72.7% and specificity about 76.5%.

Comparable to our findings, Zhu, Qingqiang et al. 2019 mentioned that the f and D values were high within CCRCCs, moderate within ChRCCs and low within PRCC. The D values of CCRCCs showed significant statistical difference among ChRCCs and PRCCs ($P<0.05$) with f and D measurements of 0.41 and 1.10, respectively, as the cutoff value for distinguishing CCRCCs versus both PRCCs and ChRCCs [22].

Our results detected that the CCRCCs had also the greatest D* values, but moderate values were detected among PRCCs and least values detected among ChRCCs. Significant statistical difference was detected among CCRCCs & ChRCCs types as well as among PRCCs & ChRCCs ($P<0.001$ for both). However, no significant statistical difference was detected among CCRCCs & PRCCs ($p=0.084$) with best detected cutoff value to differentiate CCRCCs from ChRCCs and PRCCs that is ≤ 0.0355 (AUC = 0.745) yielding sensitivity of 57.5% and specificity 83.3%. D* values may be influenced by capillary density and vascular perfusion. The tissue capillary density is probably the reason for rising D* values as clear cell RCCs are hypervascular renal tumors [23].

Our results are on the same level of agreement with **Ding, Yuqin, et al.,2016 study**; they mentioned that the three subtypes of RCCs had significant statistical difference for D* and D (all $p<0.050$) and also mentioned that CCRCCs exhibited the greatest D values. Regarding the f values their results suggested that CCRCCs had greater f values in comparison with non-CCRCCs ($p<0.05$) [24]. Contrary to our findings **Chandarana, Hersh, et al.,2012**, they reported that f parameter had higher accuracy versus D parameter (AUC = 0.74) to diagnose clear cell type, but the utilization and measurements of both f and D parameters together had the greatest accuracy (AUC = 0.78) [25].

Our research is subject to some limitations: First, the number of cases was not large and only limited number of cases enrolled within every subgroup, this might influence the reproducibility and validity of the findings, so larger sample size may be necessary to ensure our results. Second, the cases enrolled in the study were not reflective of majority of people because the research had enrolled only patients who were referred to a specialized center, which may have resulted in a biased sample. Third, there was a possibility of false(-ve) results as we might miss small foci of the tumor. Finally, our study may have lacked continuous surveillance to assess patients' clinical outcomes. For example, the study may have assessed the diagnostic accuracy of IVIM, but not its ability to predict the prognosis.

In summary, this study clarified that IVIM parameters differ significantly among renal cell carcinoma subtypes. This approach may be used as a non-invasive technique for differentiating between renal cell cancer subtypes. Even so, we cannot replace percutaneous biopsy by these radiological findings as there is major overlapping among different renal tumors.

Conclusions

In conclusion, the current study showed that IVIM quantitative parameters show the potential to favor the RCC diagnosis and characterization. It may be a hopeful method for assessment of the pathological alterations of RCC tissue, such as predict CCRCC versus non-CCRCC subtypes.

The current study has found that D value varies majorly among different subtypes of CCRCC which may reflect differences in tissue microstructure and cellular density between them and can be elucidated with RCC hypercellularity. IVIM, when used with routine MRI of kidney may be valuable in improving the specificity and the sensitivity of detection of RCC particularly combined D, D* & f showed good to excellent non-invasive diagnostic accuracy in differentiating subtypes of RCC potentially reducing the need for invasive procedures such as biopsies.

Abbreviations

RCC	Renal cell carcinoma
MRI	Magnetic resonance image
IVIM	Intravoxel incoherent motion

DWI	Diffusion-weighted images
CCRCC	Clear cell renal cell carcinoma
PRCC	Papillary renal cell carcinoma
ChRCC	Chromophobe renal cell carcinoma
WHO	World Health Organization
D	True diffusion coefficient
D*	Pseudo-diffusion
F	Perfusion fraction
ADC	Apparent diffusion coefficient
US	Ultrasound
CT	Computed tomography
FOV	Field of view
TE	Echoe time
TR	Repetition time
ROI	Region of interest
AUC	Area under the curve

Acknowledgements
We acknowledge all members of the Radiology Department in Urology and Nephrology Center, Mansoura University, Egypt.

Author contributions
AM contributed to the data collection. AM and AE performed data analysis and writing. AE, NF and EH performed supervision. They all approved the final revision of the manuscript.

Funding
This study had no funding from any resource.

Availability of data and materials
The datasets used and/or analyzed during the current study are available from the corresponding author on reasonable request.

Declarations

Ethics approval and consent to participate
This study was approved by the Research Ethics Committee of the Faculty of Medicine at Mansoura University in Egypt on 06/03/2023; reference number of approval: (MS.23.02.2297).

Consent for publication
All patients included in this research gave written informed consent to publish the data contained within this study.

Competing interests
The authors declare that they have no competing interests.

Received: 3 June 2024 Accepted: 24 August 2024
Published online: 16 September 2024

References

1. Siegel RL, Miller KD, Jemal A (2018) Cancer statistics. CA Cancer J Clin 68(1):7–30
2. Wang W, Cao K, Jin S, Zhu X, Ding J, Peng W et al (2020) Differentiation of renal cell carcinoma subtypes through MRI-based radiomics analysis. Eur Radiol 30:5738–5747
3. Armstrong AJ, Halabi S, Eisen T, Broderick S, Stadler WM, Jones RJ et al (2016) Everolimus versus sunitinib for patients with metastatic non-clear cell renal cell carcinoma (ASPEN): a multicentre, open-label, randomised phase 2 trial. Lancet Oncol 17:378–388
4. Williamson SR et al (2020) Report from the International Society of Urological Pathology (ISUP) consultation conference on molecular pathology of urogenital cancers: III: molecular pathology of kidney cancer. Am J Surg Pathol 44(7):e47
5. Serter A, Onur MR, Coban G, Yildiz P, Armagan A, Kocakoc E et al (2021) The role of diffusion-weighted MRI and contrast-enhanced MRI for differentiation between solid renal masses and renal cell carcinoma subtypes. Abdom Radiol 46:1041–1052
6. Cornelis F, Grenier N (2017) Multiparametric magnetic resonance imaging of solid renal tumors: a practical algorithm. Seminars Ultrasound CT MRI 38(1):47–58
7. Elsorougy A et al (2021) Quantitative 3-tesla multiparametric MRI in differentiation between renal cell carcinoma subtypes. Egypt J Radiol Nucl Med 52(1):1–11
8. Rouvière O et al (2020) Imaging protocols for renal multiparametric MRI and MR urography: results of a consensus conference from the French Society of Genitourinary Imaging. Eur Radiol 30:2103–2114
9. Iima M (2021) Perfusion-driven intravoxel incoherent motion (IVIM) MRI in oncology: applications, challenges, and future trends. Magn Reson Med Sci 20(2):125–138
10. Pan J, Zhang H, Man F, Shen Y, Wang Y, Zhong Y, Ma L et al (2018) Measurement and scan reproducibility of parameters of intravoxel incoherent motion in renal tumor and normal renal parenchyma: a preliminary research at 3.0 T MR. Abdom Radiol 43:17391748
11. Zhu Q, Zhu W, Ye J, Wu J, Chen W, Hao Z et al (2019) Value of intravoxel incoherent motion for differential diagnosis of renal tumors. Acta Radiol 60:382–387
12. Chandarana H, Rosenkrantz AB, Mussi TC, Kim S, Ahmad AA, Raj SD et al (2012) Histogram analysis of whole-lesion enhancement in differentiating clear cell from papillary subtype of renal cell cancer. Radiology 265:790–798
13. Shubert-Franczak AE et al (2020) Intravoxel incoherent motion magnetic resonance imaging: basic principles and clinical applications. Pol J Radiol 85(1):624–635
14. Spannuth WA, Sood AK, Coleman RL (2008) Angiogenesis as a strategic target for ovarian cancer therapy. Nat Clin Pract Oncol 5:194–204
15. Low G, Huang G, Fu W, Moloo Z, Girgis S et al (2016) Review of renal cell carcinoma and its common subtypes in radiology. World J Radiol 8:484–500
16. Lopes Vendrami C, Parada Villavicencio C, DeJulio TJ, Chatterjee A, Casalino DD, Horowitz JM et al (2017) Differentiation of solid renal tumors with multiparametric MR imaging. Radiographics 37(7):2026–2042
17. De Leon AD, Kapur P, Pedrosa I (2019) Radiomics in kidney Cancer: MR imaging. Magn Reson Imaging Clin 27(1):1–13
18. Li YT, Cercueil JP, Yuan J et al (2017) Liver intravoxel incoherent motion (IVIM) magnetic resonance imaging: a comprehensive review of published data on normal values and applications for fibrosis and tumor evaluation. Quant Imaging Med Surg 7:59–78
19. Hsieh JJ et al (2018) Genomic classifications of renal cell carcinoma: A critical step towards the future application of personalized kidney cancer care with pan-omics precision. J Pathol 244(5):525–537
20. Eckerbom P, Hansell P, Bjerner T et al (2013) Intravoxel incoherent motion MR imaging of the kidney: pilot study. Adv Exp Med Biol 765:55–58
21. Koh MJ, Lim BJ, Choi KH et al (2013) Renal histologic parameters influencing postoperative renal function in renal cell carcinoma patients. Korean J Pathol 47:557–562
22. Zhu Q et al (2019) Value of intravoxel incoherent motion for differential diagnosis of renal tumors. Acta Radiol 60(3):382–387
23. Wang H, Cheng L, Zhang X (2010) Renal cell carcinoma: diffusion-weighted MR imaging for subtype differentiation at 3.0 T. Radiology 257:135–143
24. Ding Y et al (2016) Comparison of biexponential and monoexponential model of diffusion-weighted imaging for distinguishing between common renal cell carcinoma and fat poor angiomyolipoma. Korean J Radiol 17(6):853
25. Chandarana H et al (2012) Diffusion-weighted intravoxel incoherent motion imaging of renal tumors with histopathologic correlation. Invest Radiol 47(12):688–696

Publisher's Note